Structural Aspects of the β-Polymorph of (*E*)-4-Formylcinnamic Acid: Structure Determination Directly from Powder Diffraction Data and Elucidation of Structural Disorder from Solid-State NMR

by **Siwaporn Meejoo**, **Benson M. Kariuki**, **Simon J. Kitchin**, **Eugene Y. Cheung**, **David Albesa-Jové**, and **Kenneth D. M. Harris***

School of Chemical Sciences, University of Birmingham, Edgbaston, Birmingham B15 2TT, United Kingdom (e-mail: K.D.M.Harris@bham.ac.uk)

Dedicated to Professor *Jack Dunitz*, *FRS*, on the occasion of his 80th birthday

Among the derivatives of (*E*)-cinnamic acid for which the solid-state photochemical properties have been studied, (*E*)-4-formylcinnamic acid (**1**) has already received much attention. Given the inability to prepare single crystals of the β-polymorph of **1** that are of suitable size and quality for structural characterization by single-crystal X-ray diffraction, the structure of this material was determined directly from powder X-ray-diffraction data by means of the genetic-algorithm technique for structure solution, followed by *Rietveld* refinement. High-resolution solid-state ^{13}C-NMR was also applied to elucidate details of structural disorder concerning the orientation of the formyl group, and provided independent support for the disorder model established form the *Rietveld* refinement. The reported structure establishes that the β-phase of **1** is not structurally anomalous among photoreactive (*E*)-cinnamic acid crystals, and finally resolves a long-standing controversy concerning the structural properties of this material.

1. Introduction. – The phenomenon of polymorphism [1–4] arises when members of a set of crystalline materials have the same chemical composition but different crystal structures. In the case of molecular solids, polymorphism arises when a given type of molecule is able to form different crystal structures. Although each polymorph contains the same molecule, the solid-state properties of the different polymorphs can differ substantially as a consequence of their different structural properties, and a clear illustration of this fact is provided by the photoreactivity of (*E*)-cinnamic acid (=(2*E*)-3-phenylprop-2-enoic acid) and its derivatives. Many of these materials exhibit polymorphism, with the different polymorphic forms exhibiting substantially different photoreactivities.

From extensive studies of the [2+2] photodimerization reactions of (*E*)-cinnamic acid and its derivatives [5–7], it has been found that crystals of these materials can be classified, as α-, β-, or γ-types according to their behavior in these reactions. Thus, UV irradiation of α-type crystals produces a centrosymmetric (α-truxillic acid = (1α,2α,3β,4β)-2,4-diphenylcyclobutane-1,3-dicarboxylic acid) dimer, UV irradiation of β-type crystals produces a mirror-symmetric (β-truxinic acid = (1α,2α,3β,4β)-3,4-diphenylcyclobutane-1,2-dicarboxylic acid) dimer, whereas no reaction occurs when γ-type crystals are exposed to UV radiation. The single-crystal X-ray-diffraction studies of *Schmidt* [8] demonstrated well-defined correlations between crystal structure and photoreactivity in these materials, with the α-, β-, and γ-type crystals each having a

characteristic mode of molecular packing. A general observation resulting from these studies was that, for all photoreactive (α-type and β-type) crystals, the distance between the C=C bonds of potentially reactive monomer molecules is less than *ca.* 4.2 Å, whereas the corresponding distance in all photostable (γ-type) crystals is greater than *ca.* 4.7 Å. On the basis of these well-defined structure-reactivity correlations, the photodimerization reactions in (*E*)-cinnamic acid and its derivatives represent a classic illustration of the topochemical principle [9–17], according to which the product obtained in the solid-state reaction can be rationalized on the basis of knowledge of the spatial arrangement of molecules in the reactant crystal.

In this paper, we focus on (*E*)-4-formylcinnamic acid (**1**; *Fig. 1*), which is known [18–22] to exist in two different polymorphic forms. Crystallization from EtOH produces a photoreactive β-phase (yielding 4,4′-diformyl-β-truxinic acid (=(1α,2α,3β,4β)-3,4-bis(4-formylphenyl)cyclobutane-1,2-dicarboxylic acid) on UV irradiation), whereas crystallization from acetone produces a photostable γ-phase. The structure of a crystal of **1** grown by vacuum-sublimation techniques has been reported previously [23], and was claimed to represent the crystal structure of the β-phase. If this claim were correct, this crystal structure would be of considerable interest among β-type (*E*)-cinnamic acid derivatives since the shortest distance between the C=C bonds of potentially reactive molecules of **1** in this structure is 4.825 Å. As noted above, the corresponding distance in all photoreactive (α-type and β-type) crystals of (*E*)-cinnamic acid derivatives of known structure is less than *ca.* 4.2 Å. The crystal structure reported to be the β-phase of **1** was, thus, widely accepted [17][24–30] as a structurally anomalous β-type (*E*)-cinnamic acid derivative, with an unprecedentedly (and uniquely) large value for the shortest distance between the C=C bonds of potentially reactive molecules. However, it was shown subsequently [31] that the powder X-ray-diffraction pattern calculated using the crystal structure reported [23] to be the β-phase of **1** was actually in agreement with the experimental powder X-ray-diffraction pattern of the photostable γ-phase, establishing that the crystal structure reported to be the β-phase of **1** was actually that of the γ-phase. This structure, therefore, did *not* represent a structurally anomalous photoreactive (*E*)-cinnamic acid derivative as the distance (4.825 Å) between the C=C bonds of potentially reactive molecules is within the well-established range for γ-type crystals.

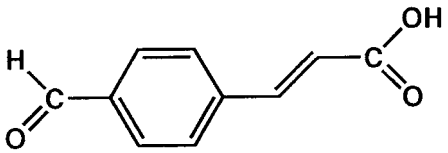

1

Fig. 1. *Structural formula of (*E*)-4-formylcinnamic acid* (**1**)

However, while the powder X-ray-diffraction study [31] established that the structure reported in [15] actually represents the γ-phase of **1**, rather than the claimed β-phase, it did not shed any light on the actual structure of the β-phase of **1**. Given the inability to prepare crystals of this material of suitable size and quality for single-crystal X-ray-diffraction studies, we have carried out structure determination of this material

directly from powder diffraction data, exploiting recently developed opportunities, reviewed elsewhere [32], in this field.

2. Background. – Among recent developments in techniques for solving crystal structures directly from powder diffraction data, the 'direct-space' strategy [33] is particularly suitable in the case of molecular materials. In this strategy, trial structures are generated in direct space, with the quality of each trial structure assessed by direct comparison between the powder diffraction pattern calculated for the trial structure and the experimental powder diffraction pattern (in our work, this comparison is made by using the powder profile *R*-factor R_{wp}, which implicitly takes peak overlap into consideration). In the present paper, direct-space structure solution was carried out using our genetic-algorithm (GA) method [34–37] to locate the trial structure corresponding to the global minimum in R_{wp}. In this method, a population of trial structures is allowed to evolve subject to rules and operations (mating, mutation, and natural selection) analogous to those that govern evolution in biological systems. Each structure in the population is specified by its 'genetic code', which represents, for each molecule in the asymmetric unit, the position $\{x, y, z\}$ and orientation $\{\theta, \phi, \psi\}$ of the molecule, and the molecular conformation (defined by variable torsion angles $\{\tau_1, \tau_2, \ldots, \tau_n\}$). The quality ('fitness') of each structure in the population is assessed from its value of R_{wp}. New structures are generated by the mating and mutation operations, and, in our implementation used here, each new structure is subjected to local minimization of R_{wp}. In the natural-selection procedure, only the structures of highest fitness (*i.e.*, lowest R_{wp}) are allowed to pass from one generation to the next generation. In the GA calculation, the population is allowed to evolve for a specified number of generations or until convergence is reached. Full details of the GA technique for structure solution are given elsewhere [34–37]. The best structure solution obtained in the GA structure-solution calculation is used as the starting structural model for *Rietveld* refinement.

3. Experimental. – The β-phase of **1** was prepared by crystallization from EtOH, with the soln. cooled from 50° to 20° within 3 days and left at 20° for 15 days before collecting the crystals. By comparison of the powder X-ray-diffraction pattern with those reported previously [31], the sample obtained in this preparation was clearly a monophasic sample of the β-phase of **1**, and no detectable impurity amount of the γ-phase was present. High-quality powder X-ray-diffraction data for this sample of the β-phase of **1** were recorded at r.t. in transmission mode on a *Siemens D5000* diffractometer (Cu$K\alpha$1 (Ge-monochromated); linear position-sensitive detector covering 8° in 2θ; 2θ range 5°–60°; step size 0.0194°; data-collection time 10 h).

High-resolution solid-state ^{13}C-NMR experiments were carried out at 75.4 MHz on a *Chemagnetics CMX-Infinity-300* spectrometer. Spectra were recorded at 25° with a *Chemagnetics* 7.5-mm probe under conditions of $^{13}C \leftarrow {}^{1}H$ cross-polarization, magic-angle sample spinning (spinning frequency 5000 ± 3 Hz), spinning sideband suppression by using the total suppression of spinning sidebands (TOSS) technique [38][39], and high-power ^{1}H-TPPM decoupling (field strength *ca.* 63 kHz). Spectra were recorded for different values of the cross-polarization contact time in the range 0.5 ms to 12 ms. The spectra are referenced relative to $SiMe_4$ (=0 ppm).

4. Structure Determination, Results, and Discussion. – The powder X-ray-diffraction pattern was indexed using the program ITO [40], leading to the following unit cell with monoclinic metric symmetry; $a = 3.89$ Å, $b = 6.83$ Å; $c = 31.76$ Å, $\beta = 87.64°$ ($V = 841.8$ Å^3). Using this unit cell in *Pawley* fitting [41] of the powder diffraction pattern (employing the PowderFit program [42] in Materials Studio [43]) resulted in a very good fit to the complete powder diffraction pattern. From systematic

absences, the space group was assigned as $P2_1/n$. Density considerations indicate that there is one molecule in the asymmetric unit (with four molecules in the unit cell, the predicted density is 1.39 g cm^{-3}, which is consistent with typical densities of organic materials).

Structure solution from the powder X-ray-diffraction data was carried out using our genetic-algorithm (GA) technique [35] within the program EAGER [44]. In the structure-solution calculation, the 'structural fragment' comprised one complete molecule of **1** with H-atoms omitted, and each structure was defined by eight variables $\{x, y, z, \theta, \phi, \psi, \tau_1, \tau_2\}$. The two variable torsion angles corresponded to rotation about the two C–C bonds attached directly to the benzene ring. The GA structure-solution calculation involved the evolution of a population of 100 structures, with 50 mating operations (to produce 100 offspring) and 20 mutation operations carried out in each generation. In the mating procedure, pairs of parents were selected from the population with a probability proportional to their fitness, and the eight variables from each parent were distributed between the two offspring such that four variables were passed from each parent to each offspring. In the mutation procedure, individual structures were selected at random from the population, and random changes were made to four variables.

The best structure solution obtained in the GA calculation was used as the starting structural model for *Rietveld* refinement, which was carried out using the GSAS program [45]. Initially, rigid-body refinement was carried out, in which the position and orientation of the rigid molecule and an overall isotropic displacement parameter were refined. Then, the rigid-body constraint was removed and the refinement proceeded with bond lengths and bond angles restrained to standard values and with planar restraints applied. These restraints were gradually relaxed as the refinement progressed. In the final refinement calculations, H-atoms were introduced in idealized positions riding on the respective C- and O-atoms, with C–H and O–H bond lengths appropriate for the atom hybridization. A common isotropic displacement parameter (final value $U_{iso} = 0.082(2)$ Å^2) was refined for all atoms. In the final stage of *Rietveld* refinement, a preferred orientation parameter was also refined.

During the refinement, we investigated the possibility that there may be disorder involving the CHO group, since this group could, in principle, be oriented in two different ways while maintaining the planarity of the molecule. Thus, a disorder model containing both orientations of the CHO group was considered, and the relative occupancies of the two orientations were refined (with the total occupancy fixed at 1). The refinement suggested that there is a higher occupancy for one orientation, with refined pupulations of 0.59(1) for the major orientation and 0.41(1) for the minor orientation. It is noteworthy that, for the major orientation, the O-atom of the CHO group is engaged in a short intermolecular C–H$\cdots$O contact [46][47], whereas there is no short contact of this type for the minor orientation. Refinement calculations were also carried out for two ordered models comprising only the major orientation and only the minor orientation of the CHO group, respectively. Although the quality of fit to the powder diffraction data obtained for the disordered model (*Fig. 2*; $R_{wp} = 2.87\%$) is better than those obtained for the two ordered models (*Fig. 3*; $R_{wp} = 3.27\%$ (major orientation only), $R_{wp} = 3.75\%$ (minor orientation only)), the improvement in the quality of fit obtained with the disordered model is not substantial, and, therefore, we

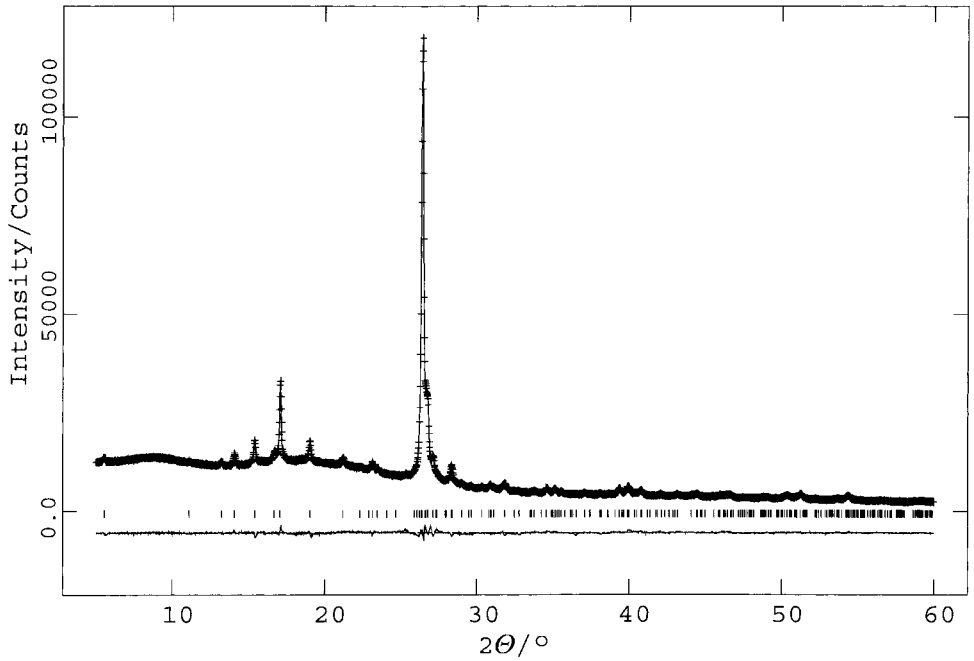

Fig. 2. *Experimental* (+ marks), *calculated* (solid line), *and difference* (bottom) *powder diffraction profiles for the* Rietveld *refinement of the β-phase of* **1** ($R_{wp}=2.87\%$; $R_p=2.00\%$). Reflection positions are marked. The calculated powder diffraction profile is for the final refined crystal structure, including disorder of the CHO group.

sought independent evidence for the existence of disorder in this structure using high-resolution solid-state ^{13}C-NMR spectroscopy.

The high-resolution solid-state ^{13}C-NMR spectrum of the β-phase of **1** is shown in *Fig. 4*. Importantly, in the region of the spectrum corresponding to the C-atom of the CHO group, two isotropic peaks are observed (at 191.4 and 193.0 ppm). For all other C-atoms in the molecule, only one isotropic peak is observed, consistent with the fact that there is one molecule in the asymmetric unit in the structure. Furthermore, under the conditions of the measurements, there is no NMR interaction that would give rise to splitting of isotropic peaks for molecule **1**. The observation of two isotropic peaks for the C-atom of the CHO group can be rationalized in terms of the material containing two different local structural environments for this group, as in the disorder model discussed above. The orientation with higher isotropic ^{13}C chemical shift (193.0 ppm) can be assigned as the orientation in which the CHO group is engaged in a short intermolecular C–H···O contact, on the basis of the fact that intermolecular H-bonding to carbonyl groups is known to increase the isotropic ^{13}C chemical shift. The high-resolution solid-state ^{13}C-NMR spectrum shown in *Fig. 4* was recorded under conditions of ^{13}C ← ^{1}H cross-polarization, and, therefore, a single spectrum of this type cannot necessarily be interpreted on a quantitative basis, and analysis of a series of such spectra recorded as a function of cross-polarization contact time (τ_{cp}) are required to

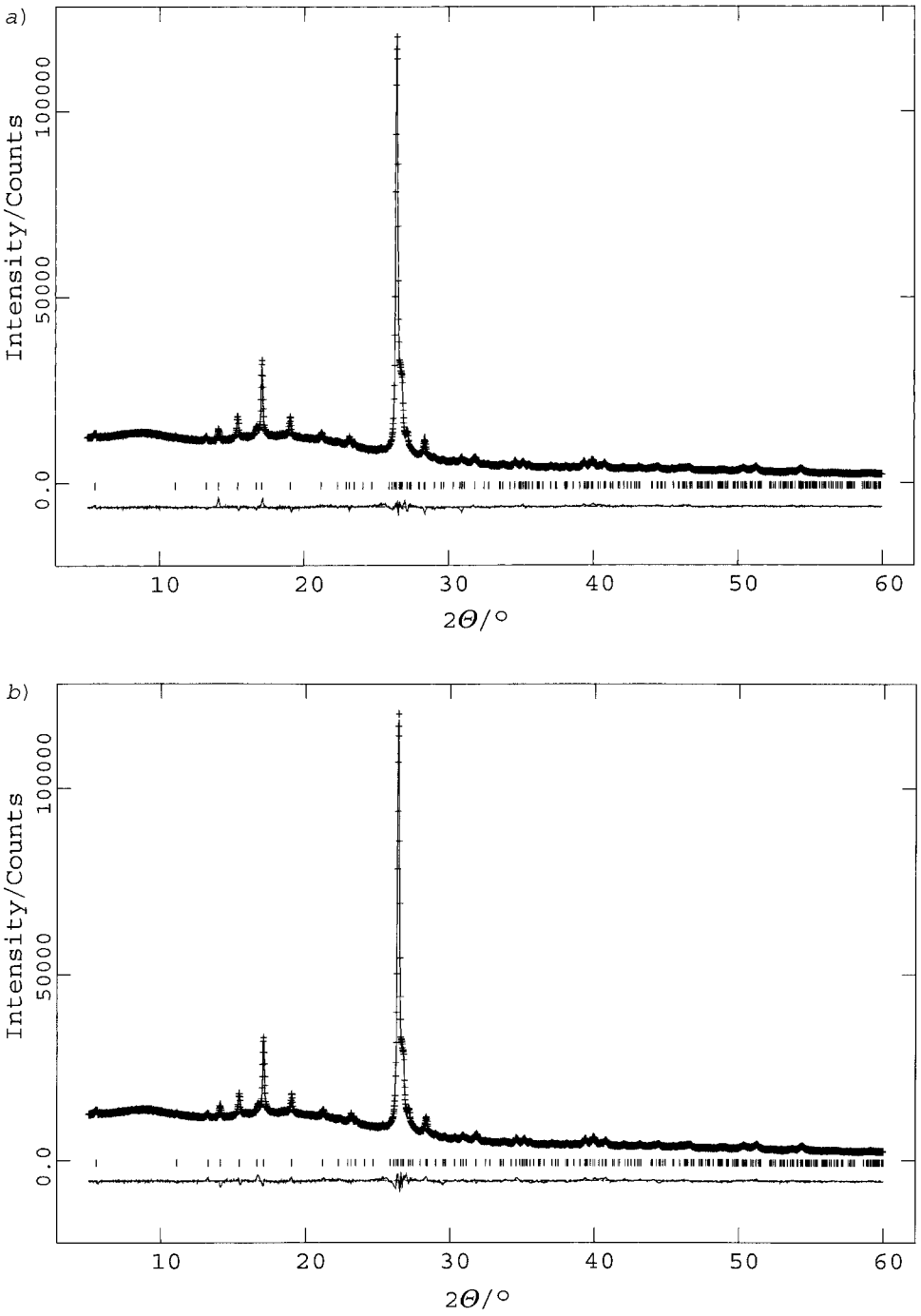

Fig. 3. *Powder diffraction profiles for the* Rietveld *refinement of the β-phase of* **1** *for ordered models of the CHO group comprising* a) *only the major orientation* ($R_{wp}=3.27\%$; $R_p=2.15\%$) *and* b) *only the minor orientation* ($R_{wp}=3.75\%$; $R_p=2.55\%$). Apart from the description of the order/disorder of the CHO group, all other aspects of these refinement calculations were the same as that shown in *Fig. 2* for the disordered model.

quantify this issue. In the present case, the relative intensities of the two peaks for the CHO group were found to be independent of the contact time, and corresponded (*via* lineshape fitting) to relative populations of 0.69 and 0.31 for the two orientations, with the peak at 193.0 ppm representing the higher population. Thus, in agreement with the results from *Rietveld* refinement, the orientation that has the intermolecular C–H···O interaction has the higher population. Within reasonable experimental errors, the population ratios obtained from the solid-state ^{13}C-NMR data and from the *Rietveld* refinement are also in close agreement (in this regard, we note that the estimated standard deviations (0.01) in the occupancies refined from the powder diffraction data reflect more the precision in the refinement procedure, rather than the absolute accuracy in the refined value).

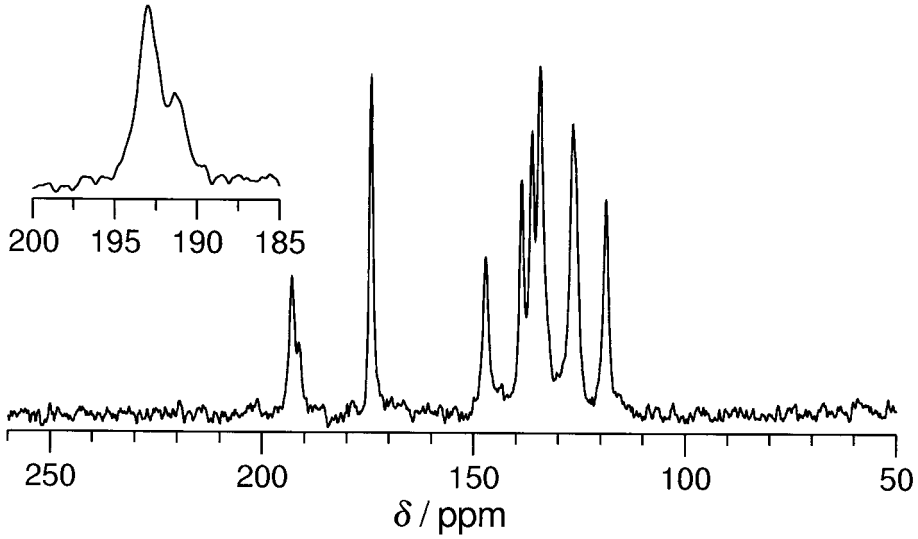

Fig. 4. *High-resolution solid-state ^{13}C-NMR spectrum recorded for the β-phase of* **1** (cross-polarization contact time 2 ms). The inset shows the region of the spectrum corresponding to the CHO group.

Our *Rietveld* refinement calculations also explored whether the C–O bond lengths in the carboxylic acid group were equal (representing disorder involving two orientations of the COOH group, as often observed for carboxylic acid dimers) or different (representing distinguishable C–OH single and C=O double bonds), although no significant discrimination was obtained. The disordered model (with the H-atom included at two positions with half occupancy) was used in the final refinement calculations.

The final *Rietveld* refinement (*Fig. 2*), for the structural model with disorder of the CHO group as discussed above, gave $R_{wp} = 2.87\%$ and $R_p = 2.00\%$ for 364 reflections and 2836 data points, with 81 refined parameters and 61 geometric restraints. The final refined structure is shown in *Fig. 5*, and fractional atomic coordinates are given in the *Table*.

The crystal structure of the β-phase of **1** contains pairs of molecules linked by H-bonding of their carboxylic acid groups, involving two O–H···O H-bonds (O···O

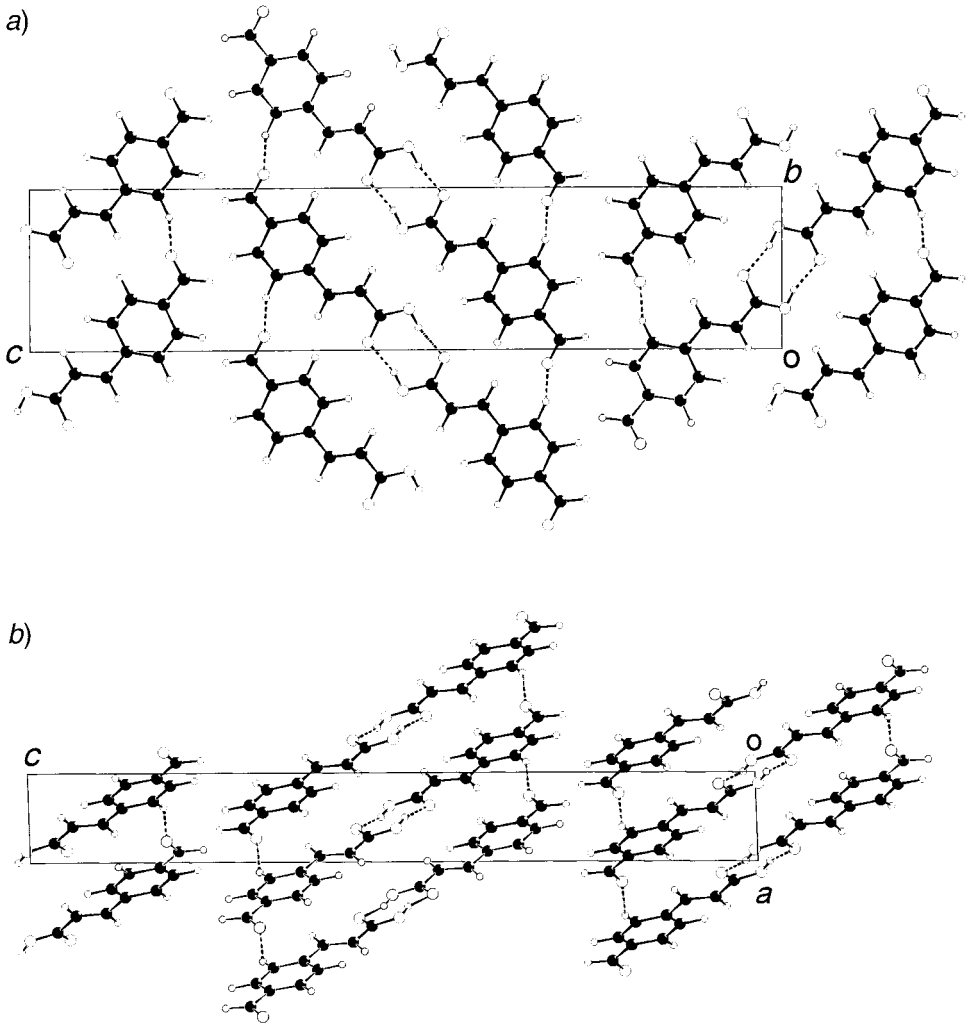

Fig. 5. *Final refined structure of the β-phase of* **1** *viewed* a) *along the* a-*axis and* b) *along the* b-*axis*. Only the major orientation of the CHO group is shown, and the dotted line represents the C–H···O interaction that occurs for this orientation of the CHO group. For the CO_2H group, only one position of the H-atom is indicated.

distances 2.70(1) Å) in the commonly observed eight-membered ring $R_2^2(8)$ motif. The molecules form stacks along the *a*-axis (the shortest unit-cell axis). Adjacent molecules along the stack are related by translation, with a distance of 3.89(1) Å between the centres of the C=C bonds of adjacent molecules. In addition, as noted above, the CHO group is disordered between two orientations, and in the orientation of higher population, the O-atom forms a short intermolecular C–H···O contact (C···O, 3.18(1) Å; C–H···O, 147.0(6)°) involving a C–H bond of the benzene ring of a neighboring molecule (in a different stack). It is clear that potentially photodimeriz-

Table 1. *Fractional Atomic Coordinates in the Final Refined Structure of the β-Phase of* **1**. Space group $P2_1/n$; final refined lattice parameters: $a = 3.8881(3)$ Å, $b = 6.8329(9)$ Å, $c = 31.8065(67)$ Å, $\beta = 92.120(7)°$; $V = 844.4(3)$ Å^3.

Atom	*x*/*a*	*y*/*b*	*z*/*c*	Occupancy
O(1)	1.2338(22)	0.4123(11)	0.18826(31)	0.589(11)
C(2)	1.1201(12)	0.5562(11)	0.20469(24)	1
C(3)	0.9422(11)	0.7130(8)	0.17790(18)	1
C(4)	0.8784(13)	0.6811(7)	0.13490(19)	1
C(5)	0.7093(16)	0.8239(7)	0.11041(15)	1
C(6)	0.8595(14)	0.8929(9)	0.19577(15)	1
C(7)	0.6870(16)	1.0350(8)	0.17143(14)	1
C(8)	0.6131(11)	1.0008(6)	0.12866(14)	1
C(9)	0.4338(12)	1.1576(7)	0.10187(15)	1
C(10)	0.4040(14)	1.1363(7)	0.06010(15)	1
C(11)	0.2175(12)	1.2868(6)	0.03409(16)	1
O(12)	0.1246(18)	1.2486(8)	−0.00430(19)	1
O(13)	0.1343(16)	1.4513(7)	0.05077(22)	1
O(14)	1.1431(23)	0.5743(14)	0.24252(25)	0.411(11)
H(15)	1.1410(23)	0.5728(13)	0.23876(25)	0.589(11)
H(16)	0.9488(22)	0.5420(8)	0.12082(23)	1
H(17)	0.6526(21)	0.7973(9)	0.07709(19)	1
H(18)	0.9129(21)	0.9185(12)	0.22920(18)	1
H(19)	0.6162(22)	1.1739(10)	0.18554(17)	1
H(20)	0.3285(32)	1.2871(10)	0.11679(19)	1
H(21)	0.5059(29)	1.0060(9)	0.04520(17)	1
H(22)	0.0036(24)	1.3623(12)	−0.01639(21)	0.5
H(23)	0.0111(24)	1.5312(11)	0.02952(26)	0.5
H(24)	1.2244(24)	0.4265(11)	0.18985(30)	0.411(11)

able pairs of molecules are related by translation along the *a*-axis. Thus, based on topochemical arguments, photodimerization in this material should produce the mirror symmetric (*β*-truxinic acid) dimer, as observed in practice [18–22].

5. Concluding Remarks. – The structure reported here for the *β*-phase of **1** is completely in line with the structural characteristics reported for other *β*-phase derivatives of (*E*)-cinnamic acid. This work has, thus, resolved the structural controversy that has surrounded this material, and establishes that, contrary to a previous report [23], the *β*-phase of **1** is *not* structurally anomalous among photoreactive (*E*)-cinnamic acid crystals. The elucidation of the structural disorder involving the orientation of the formyl group in this material highlights the advantages of tackling such issues by applying both diffraction-based techniques and solid-state NMR spectroscopy in conjunction with one another.

In addition, this work demonstrates the opportunity to exploit powder X-ray-diffraction techniques for carrying out complete structure determination of molecular solids when single crystals suitable for single-crystal X-ray diffraction cannot be prepared. In view of the fact that many solid-state reactions proceed from a single crystal of reactant to a polycrystalline product phase, there is considerable opportunity, which we are currently exploring, to exploit powder diffraction techniques for carrying out structure determination of the product (dimer) phases produced directly in such

reactions. Such studies are particularly pertinent in the case of the β-phase of **1**, for which it has been reported [18][19] that the photodimerization reaction is associated with uptake of H_2O by the material. Clearly, knowledge of the crystal structure of the reactant phase reported here, together with knowledge of the structural properties of the product phase (work currently in progress), should provide an opportunity to understand this interesting aspect of the photodimerization reaction in this system.

We are grateful to *EPSRC*, the University of Birmingham, and *Proctor & Gamble Inc.* for financial support, and to the *Development and Promotion of Science and Technology Talents Project* (DPST) of Thailand for a studentship to *S. M.* We are grateful to Professor Sir *John Meurig Thomas*, *FRS*, for inspiring our initial interest in the solid state chemistry and photochemistry of cinnamic acids.

REFERENCES

[1] J. D. Dunitz, *Pure Appl. Chem.* **1991**, *63*, 177.
[2] M. R. Caira, *Top. Curr. Chem.* **1998**, *198*, 164.
[3] J. Bernstein, R. J. Davey, J.-O. Henck, *Angew. Chem., Int. Ed.* **1999**, *38*, 3441.
[4] J. Bernstein, 'Polymorphism in Molecular Crystals', Oxford University Press/International Union of Crystallography, Oxford, 2002.
[5] A. Mustafa, *Chem. Rev.* **1952**, *51*, 1.
[6] M. D. Cohen, G. M. J. Schmidt, F. I. Sonntag, *J. Chem. Soc.* **1964**, 2000.
[7] G. M. J. Schmidt, in 'Reactivity of the Photoexcited Molecule', Interscience, New York, 1967, p. 227.
[8] G. M. J. Schmidt, *J. Chem. Soc.* **1964**, 2014.
[9] V. Kohlschutter, J. L. Tuscher, *Z. Anorg. Allg. Chem.* **1920**, *111*, 193.
[10] M. D. Cohen, G. M. J. Schmidt, *J. Chem. Soc.* **1964**, 1996.
[11] F. L. Hirschfeld, G. M. J. Schmidt, *J. Polym. Sci. Part A* **1964**, *2*, 2181.
[12] M. D. Cohen, *Pure Appl. Chem.* **1964**, *9*, 567.
[13] G. M. J. Schmidt, *Pure Appl. Chem.* **1971**, *27*, 647.
[14] J. M. Thomas, *Phil. Trans. Royal Soc.* **1974**, *277*, 251.
[15] M. D. Cohen, *Angew. Chem., Int. Ed.* **1975**, *14*, 386.
[16] J. M. Thomas, *Pure Appl. Chem.* **1979**, *51*, 1065.
[17] M. Hasegawa, *Pure Appl. Chem.* **1986**, *58*, 1179.
[18] F. Nakanishi, H. Nakanishi, T. Tasai, Y. Suzuki, M. Hasegawa, *Chem. Lett.* **1974**, 525.
[19] F. Nakanishi, H. Nakanishi, M. Tsuchiya, M. Hasegawa, *Bull. Chem. Soc. Jpn.* **1976**, *49*, 3096.
[20] M. Hasegawa, H. Katsuki, Y. Iida, *Chem. Lett.* **1981**, 1799.
[21] U. Ghosh, T. N. Misra, *Bull. Chem. Soc. Jpn.* **1985**, *58*, 2403.
[22] K. D. M. Harris, J. M. Thomas, *J. Solid State Chem.* **1991**, *93*, 197.
[23] H. Nakanishi, M. Hasegawa, T. Mori, *Acta Crystallogr., Sect. C* **1985**, *41*, 70.
[24] V. Ramamurthy, *Tetrahedron* **1986**, *42*, 5753.
[25] G. S. Murthy, P. Arjunan, K. Venkatesan, V. Ramamurthy, *Tetrahedron* **1987**, *43*, 1225.
[26] S. Garcia-Granda, G. Beurskens, P. T. Beurskens, T. S. R. Krishna, G. R. Desiraju, *Acta Crystallogr., Sect. C* **1987**, *43*, 683.
[27] V. Ramamurthy, K. Venkatesan, *Chem. Rev.* **1987**, *87*, 433.
[28] M. Nethaji, V. Pattabhi, G. R. Desiraju, *Acta Crystallogr., Sect. C* **1988**, *44*, 275.
[29] T. Iwamoto, S. Kashino, M. Haisa, *Acta Crystallogr., Sect. C* **1989**, *45*, 1753.
[30] S. Chakrabarti, M. Gantait, T. N. Misra, *Proc. Indian Acad. Sci. (Chem. Sci.)* **1990**, *102*, 165.
[31] K. D. M. Harris, I. L. J. Patterson, *J. Chem. Soc., Perkin Trans. 2* **1994**, 1201.
[32] K. D. M. Harris, M. Tremayne, B. M. Kariuki, *Angew. Chem., Int. Ed.* **2001**, *40*, 1626.
[33] K. D. M. Harris, M. Tremayne, P. Lightfoot, P. G. Bruce, *J. Am. Chem. Soc.* **1994**, *116*, 3543.
[34] B. M. Kariuki, H. Serrano-González, R. L. Johnston, K. D. M. Harris, *Chem. Phys. Lett.* **1997**, *280*, 189.
[35] K. D. M. Harris, R. L. Johnston, B. M. Kariuki, *Acta Crystallogr., Sect. A* **1998**, *54*, 632.
[36] G. W. Turner, E. Tedesco, K. D. M. Harris, R. L. Johnston, B. M. Kariuki, *Chem. Phys. Lett.* **2000**, *321*, 183.
[37] E. Tedesco, G. W. Turner, K. D. M. Harris, R. L. Johnston, B. M. Kariuki, *Angew. Chem., Int. Ed.* **2000**, *39*, 4488.

[38] W. T. Dixon, *J. Chem. Phys.* **1982**, *77*, 1800.
[39] W. T. Dixon, J. Schaefer, M. D. Sefcik, E. O. Stejskal, R. A. Mckay, *J. Magn. Reson.* **1982**, *49*, 341.
[40] J. W. Visser, *J. Appl. Crystallogr.* **1969**, *2*, 89.
[41] G. S. Pawley, *J. Appl. Crystallogr.* **1981**, *14*, 357.
[42] G. E. Engel, S. Wilke, O. König, K. D. M. Harris, F. J. J. Leusen, *J. Appl. Crystallogr.* **1999**, *32*, 1169.
[43] 'Materials Studio', Accelrys Inc., 9685 Scranton Road, San Diego, CA 9212103752, U.S.A.
[44] K. D. M. Harris, R. L. Johnston, D. Albesa Jové, M. H. Chao, E. Y. Cheung, S. Habershon, B. M. Kariuki, O. J. Lanning, E. Tedesco, G. W. Turner, 'Evolutionary Algorithm Generalized for Energy and R-Factor', University of Birmingham, Birmingham, United Kingdom, 2001 (an extended version of the program GAPSS, K. D. M. Harris, R. L. Johnston, B. M. Kariuki, University of Birmingham, 1997).
[45] A. C. Larson, R. B. Von Dreele, Los Alamos Laboratory Report No. LA-UR-86-748, 1987.
[46] P. Seiler, J. D. Dunitz, *Helv. Chim. Acta* **1989**, *72*, 1125.
[47] G. R. Desiraju, T. Steiner, 'The Weak Hydrogen Bond in Structural Chemistry and Biology', International Union of Crystallography and Oxford Science Publications, New York, 1999.

Received March 13, 2003